

Two-dimensional grating line parameter calibration based on biaxial phase mapping

TENG Hai-ruì, LIANG Xu, JIN Si-yu, SUN Yu-jia, LI Wen-hao, LIU Zhao-wu

Citation:

TENG Hai-ruì, LIANG Xu, JIN Si-yu, SUN Yu-jia, LI Wen-hao, LIU Zhao-wu. Two-dimensional grating line parameter calibration based on biaxial phase mapping[J]. *Chinese Optics*, 2026, 19(2): 407–420. doi: 10.37188/CO.EN-2025-0020

滕海瑞, 梁旭, 金思宇, 孙宇佳, 李文昊, 刘兆武. 双轴相位映射的二维光栅栅线参数标校[J]. *中国光学*, 2026, 19(2): 407–420. doi: 10.37188/CO.EN-2025-0020

View online: <https://doi.org/10.37188/CO.EN-2025-0020>

Articles you may be interested in

[Influence of CCD nonlinearity effect on the three-dimensional shape measurement of dual frequency grating](#)

CCD非线性效应对双频光栅三维面形测量的影响

Chinese Optics. 2021, 14(3): 661 <https://doi.org/10.37188/CO.2020-0143>

[Progress on two-dimensional quantum sheets and their optics](#)

二维量子片及其光学研究进展

Chinese Optics. 2021, 14(1): 1 <https://doi.org/10.37188/CO.2020-0176>

[Highly sensitive infrared detector based on a two-dimensional heterojunction](#)

二维材料异质结高灵敏度红外探测器

Chinese Optics. 2021, 14(1): 87 <https://doi.org/10.37188/CO.2020-0139>

[Two-dimensional material photodetector for hybrid silicon photonics](#)

面向硅基光电子混合集成的二维材料探测器

Chinese Optics. 2021, 14(5): 1039 <https://doi.org/10.37188/CO.2021-0003>

[Progress of two-dimensional photonic topological insulators](#)

二维光子拓扑绝缘体研究进展

Chinese Optics. 2021, 14(4): 935 <https://doi.org/10.37188/CO.2021-0076>

[A fast blind denoising method for grating image](#)

针对光栅图像的快速盲去噪方法

Chinese Optics. 2021, 14(3): 596 <https://doi.org/10.37188/CO.2020-0166>

Two-dimensional grating line parameter calibration based on biaxial phase mapping

TENG Hai-rui^{1,2}, LIANG Xu¹, JIN Si-yu¹, SUN Yu-jia¹, LI Wen-hao¹, LIU Zhao-wu^{1*}

(1. *Changchun Institute of Optics, Fine Mechanics and Physics, Chinese Academy of Sciences, Changchun 130033, China;*

2. *University of Chinese Academy of Sciences, Beijing 100049, China)*

* *Corresponding author, E-mail: zhaowuliu@ciomp.ac.cn*

Abstract: The two-dimensional grating serves as a critical component in plane grating interferometers for achieving high-precision multidimensional displacement measurements. The calibration of grating groove density and orthogonality error of grating grooves not only improves the positioning accuracy of grating interferometers but also provides essential feedback for optimizing two-dimensional grating fabrication. This study proposes a method for simultaneous calibration of these parameters using orthogonal heterodyne laser interferometry. A two-dimensional grating interferometer is built with the grating to be measured, and a biaxial laser interferometer provides a displacement reference for it. The phase mapping relationship between grating interference and laser interference is established. The interference phase information obtained by any two displacements can simultaneously solve the above three parameters and obtain the grating installation error. The feasibility of the proposed method is verified by using a 1200 gr/mm two-dimensional grating. The standard deviation of the grating groove density in the X and Y directions is 0.012 gr/mm and 0.014 gr/mm, respectively. The standard deviation of the orthogonality error of grating grooves is 0.004° , and the standard deviation of the installation error is 0.002° . Compared with the atomic force microscope method, the consistency of the grating groove density in the X and Y directions is better than 0.03 gr/mm and 0.06 gr/mm, and the orthogonality error of grating grooves is better than 0.008° . The experimental results show that the proposed method can be simply and efficiently applied to the calibration of the grating line parameters of the two-dimensional grating.

Key words: two-dimensional grating; grating line parameter calibration; grating groove density; orthogonality error of grating grooves

收稿日期:2025-03-17; 修订日期:2025-04-03

基金项目:国家自然科学基金青年基金项目(No. 52305592); 国家自然科学基金(No. 62435019); 吉林省科技发展计划项目(No. 20240404065ZP, No. YDZJ202401295ZYTS, No. 20230508093RC)

Supported by Youth Fund Project of the National Natural Science Foundation of China (No. 52305592); National Natural Science Foundation (No. 62435019); Science and Technology Development Plan Project of Jilin Province (No. 20240404065ZP, No. YDZJ202401295ZYTS, No. 20230508093RC)

双轴相位映射的二维光栅栅线参数标校

滕海瑞^{1,2}, 梁旭¹, 金思宇¹, 孙宇佳¹, 李文昊¹, 刘兆武^{1*}

(1. 中国科学院长春光学精密机械与物理研究所, 吉林 长春 130033;

2. 中国科学院大学, 北京 100049)

摘要: 二维光栅是平面光栅干涉仪实现高精度、多维位移测量的核心器件, 其刻线密度和栅线正交性误差的检测与标校, 一方面可提高光栅干涉仪的定位精度, 另一方面可为二维光栅的制作提供反馈指导。本文提出一种利用正交外差激光干涉仪同时标定二维光栅刻线密度和栅线正交性误差的方法, 以待测光栅搭建二维光栅干涉仪, 双轴激光干涉仪为其提供位移参考, 建立光栅干涉与激光干涉的相位映射关系, 通过任意两次位移获取的干涉相位信息, 即可解算上述 3 项参数, 同时又可获取光栅安装误差。使用 1200 gr/mm 的二维光栅验证了提出方法的可行性, X、Y 方向刻线密度的标准差分别为 0.012 gr/mm 和 0.014 gr/mm, 栅线正交性误差的标准差为 0.004°, 安装误差标准差为 0.002°。与原子力显微镜法进行了精度比对, X、Y 方向刻线密度的一致性优于 0.03 gr/mm、0.06 gr/mm, 正交性误差优于 0.008°。实验结果表明, 本文提出的方法可简单、高效的应用于二维光栅的栅线参数标定。

关键词: 二维光栅; 栅线参数标校; 刻线密度; 栅线正交性误差

中图分类号: TP394.1; TH691.9 文献标志码: A doi: 10.37188/CO.EN-2025-0020 CSTR: 32171.14.CO.EN-2025-0020

1 Introduction

Precise displacement measurement is a prerequisite for ensuring stable operation and accurate control of moving units in equipment such as integrated circuit manufacturing apparatus, precision computer control machine tools, and coordinate measurement instruments^[1-2]. As a common basic component, the positioning performance of a two-dimensional(2D) worktable determines the processing and detection quality of the equipment. More specifically, lithography constitutes the cornerstone of integrated circuit fabrication, emerging as one of the most critical and technologically demanding steps that require nanoscale precision control. Using the 193ArF immersion step-and-scan lithography machine as an example, to fabricate 32–10 nm node chip, nanometer-level positioning accuracy must be achieved within a 400-mm-wide plane^[3]. Among the numerous planar displacement measurement solutions that are available, the mainstream options are laser interferometers^[4] and grating interferometers^[5-8]. Grating interferometers use the grating pitch as a reference, with the probe be-

ing distributed vertically along the scale grating. The spatial optical path does not vary with the stroke. When compared with laser interference measurements, the grating interferometer has a better ability to avoid environmental interference, has a compact layout, and is easy to integrate. As the core device in a grating interferometer, the grating groove density and the orthogonality error of grating grooves of the 2D grating will affect the pitch reference accuracy of the 2D grating, thus fundamentally determining its planar positioning performance. For example, when a 1200 gr/mm 2D grating has a line error of 1 gr/mm, it will cause a displacement deviation of 80 μm within a 100 mm measurement stroke. Additionally, when there is an orthogonality deviation of 20" between the XY-direction grid lines, it will cause a displacement deviation of 10 μm within a 100 mm measurement stroke^[9]. Therefore, determining how to calibrate the two error parameters above accurately will be highly significant for optimization of the 2D grating manufacturing process and for accurate analysis of the planar positioning errors of grating interferometers.

At present, the main methods used to measure the basic parameters (e.g., grating groove density,

orthogonality error of grating grooves) of grating rulings are the atomic force microscopy (AFM)^[10-12] method, the optical diffraction method^[13-14] and the laser interferometer comparison method^[15-17]. The AFM method calculates and acquires the grating groove density information by recording images of the number of periodic grids scanned by the probe and determining the moving displacement^[18-21]. Because of the large variations in the micro-morphology of the grating's periodic grids, methods such as the centroid method^[22-24], and the Fourier analysis method^[25] must be used in combination to improve the reading accuracy of the periodic grids and thus enhance the detection accuracy of the grating groove density. After acquisition of the grating groove density information for the grid lines in the two dimensions of the 2D grating and the grating groove density information for the hypotenuse rulings, the cosine theorem can then be used to determine the orthogonality angle information of the XY-direction grid lines^[26-28]. However, because it is limited by the point-by-point scanning measurement method used by the AFM, it requires an extremely long time for the measurement. Scanning a 1 mm×1 mm area may take up to 600 h^[29], thus making it difficult to apply the AFM method to the calibration of large-sized metrology gratings.

The optical diffraction method is based on the grating equation. By recording the angular changes that occur under self-collimated incidence conditions for the zeroth-order light and the m-order diffracted light using a high-precision turntable, the grating groove density can be calculated indirectly^[30-31]. Because the detection spot can cover thousands of grid lines, the influence of grid pitch nonuniformity on the grating groove density measurements can be reduced because of the averaging effect. However, the method can only measure the average grating groove density within the area covered by the spot and it cannot perform full-format measurements on large-sized metrology gratings. The National Institute of Metrology of China

developed a traceable measurement methodology employing a high-precision rotary stage to mount a two-dimensional grating. By leveraging optical diffraction principles, researchers sequentially aligned identical diffraction orders in orthogonal axes using a position-sensitive photodetector, enabling nanoradian-level quantification of grating groove orthogonality errors^[32]. Because of the effects of the beam alignment accuracy, the measurement standard deviation for this method was 0.03°. The centroid alignment repeatability accuracy of the laser spot was the largest error source in this method. To improve the angular position alignment accuracy of the orthogonal diffracted beams, Feng et al. from Tsinghua University^[33] used the interference fringes generated by diffracted beams of different orders to align the periodic direction of the grating, and then measured the orthogonality angle errors of the grid lines with an autocollimator. When measuring a 2D grating with a grid pitch of 1 μm, the standard deviation was 0.28".

The laser interferometer comparison method, which is characterized by high detection sensitivity, a large measurement range, and traceability, can be used to perform high-precision calibration of the grating groove density. The laser interferometer and the grating interferometer simultaneously detect the displacement change in the scale grating. By taking the value measured by the laser interferometer as the reference true value and then recording the number of interference fringes generated by scanning the grating, the grating groove density information can be determined directly by dividing the two values. Xie et al. from Jinan University^[34], based on the laser interferometer comparison method, maintained the phase stability of a measurement grating's interference field using interference fringe drift feedback from the reference grating, and achieved picometer-level resolution and ppm-level repeatability during grating groove density measurements. Hsu^[35] et al. fixed both the reference grating and the measurement grating rigidly, used the laser interfer-

ometer comparison method to calculate the reference grating groove density to eliminate installation errors between the grating to be measured and the motion stage, and then used the reference grating as a displacement reference to acquire the grating groove density of the grating to be measured. The measurement error when compared with the reference grating was better than 1 nm. The laser interferometer comparison method has also been used in the calibration of 2D grating rulers. Dong Xinyuan from Tianjin University^[36] proposed a method that used a biaxial orthogonal laser interferometer to calibrate the planar positioning accuracy of a 2D grating ruler, and also analyzed the effects of the straightness error of the carrier stage and the grating installation error on the calibration accuracy of the 2D grating ruler. However, they did not consider the influence of the parameter errors (e.g., grating groove density and orthogonality error of grating grooves) of the 2D grating itself on the displacement measurement results.

This paper proposes a method for simultaneous calibration of the grating groove density and the orthogonality error of grating grooves of a 2D grating. By using the grating to be measured as a scale, a 2D grating interferometer is constructed. A high-precision motion stage carries the grating to be measured to perform planar motion. A biaxial orthogonal laser interferometer is used to provide a displacement reference benchmark for the 2D grating. The laser interferometer and the grating interferometer share the same heterodyne light source and the same signal reception system to ensure the consistency and synchronism of the measurement results. A mathematical correspondence relationship is established between the grating interference phase and the laser interference phase. Using the measurement data acquired from two displacements of the grating, the grating groove density, the orthogonality error of grating grooves error, and the grating installation error can be resolved simultaneously. Calibration experiments are conducted on multiple re-

gions within the 2D grating format to verify the measurement performance of the proposed method. The measurement accuracy of this method is verified via comparison with the AFM method.

2 Structure and principle of the two-dimensional grating parameter calibration system

2.1 System optical path composition

The devices used in this system mainly include reflector mirror (M), beam splitter (BS), polarization beam splitter (PBS), commercial interferometer (10706B) and photodetector (PD). The overall optical path structure of this system, which is shown in Fig. 1 (color online), consists of two main parts: a 2D grating planar interferometer and a biaxial laser interferometer (in the figure, green light rays represent the optical path of the laser interferometer, red light rays represent the optical path of the grating displacement measurement device, and orange light rays represent the combined-beam interference optical path). The orthogonally polarized laser light emitted by the dual-frequency laser is split into two parts after passing through beam splitter BS₁. The reflected light is refracted by M₇ and M₈ and is then incident on the Y-axis laser interferometer (composed of 10706B_y and M_y), and the transmitted light is incident on the X-axis laser interferometer (composed of 10706B_x and M_x) after it passes through BS₂.

The measurement signals from the two groups of interferometers and the reference signal built into the laser are then analyzed by the data-processing board to provide a true value for the displacement reference for the 2D motion stage. The reflected light that passes through BS₂ with the reflection of M₁ and M₂ is then vertically incident on the 2D grating to be measured and undergoes diffraction. The ± 1 st-order diffracted light beams in the X-direction are combined at PBS₁ after passing through M₃ and M₄. Following polarization by the integrated linear

polarizer within the PD_{gx} module, the beams generate interference patterns, with the resultant phase-modulated signals being precisely captured through PD_{gx}. Similarly, the ± 1 st-order diffracted light beams in the Y-direction are combined at PBS₂ after passing through M₅ and M₆. After these beams are

polarized by the built-in linear polarizer, interference occurs, and the resulting signal is received by PD_{gy}. The two groups of interference signals above are then transmitted to the data-processing board to be processed, and the grating interference displacement information can then be obtained.

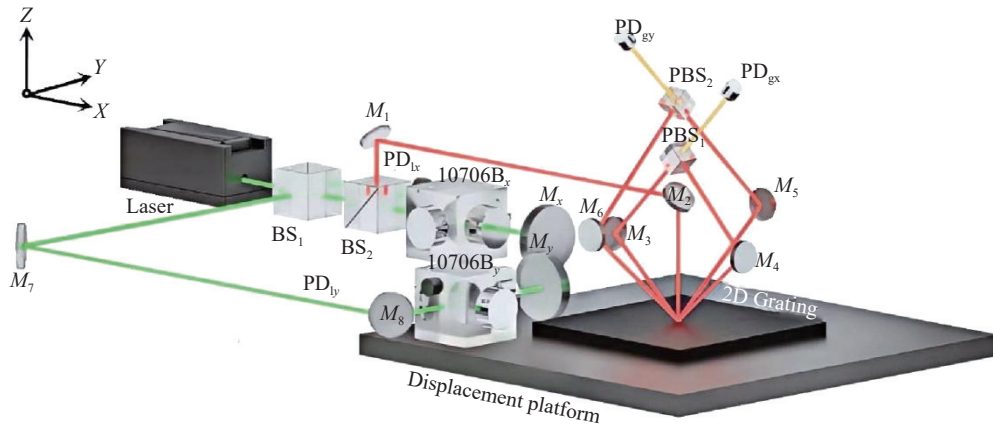


Fig. 1 Schematic diagram of the optical path structure of the calibration system

2.2 Principle of calibration for the 2D grating parameters

According to the basic principle of laser heterodyne interference, the interference signal can be expressed as:

$$I_1 \propto A_1^2 + A_2^2 + 2A_1A_2 \cos(\Delta\omega t + \Delta\varphi_0 + \varphi_1) \quad (1)$$

where A is the amplitude, $\Delta\omega$ is the angular frequency difference between the beams of the dual-frequency laser, $\Delta\varphi_0$ is the initial phase difference between the two light beams, and φ_1 is the phase change caused by the motion of the target object. The interference phase changes in the X and Y directions can be expressed, respectively, as:

$$\varphi_x = \frac{4\pi n_{\text{air}}}{\lambda} \Delta x \quad (2)$$

$$\varphi_y = \frac{4\pi n_{\text{air}}}{\lambda} \Delta y \quad (3)$$

where Δx and Δy are the displacement changes in the measurement mirrors of the laser interferometer in the 2D directions, n_{air} is the refractive index of air, and λ is the wavelength of the laser source.

The interference signal of the ± 1 st-order dif-

fracted light beams from the grating interferometer can be expressed as:

$$I_g \propto A_{+1}^2 + A_{-1}^2 + 2A_{+1}A_{-1} \cos(\Delta\omega t + \Delta\varphi_0 + \varphi_g) \quad (4)$$

where φ_g represents the interference phase change caused by the grating Doppler shift, and the phase changes in the X and Y directions can be expressed as follows:

$$\varphi_a = \int_0^t 2\pi\Delta f_a dt = 4\pi\rho_x\Delta a \quad (5)$$

$$\varphi_b = \int_0^t 2\pi\Delta f_b dt = 4\pi\rho_y\Delta b \quad (6)$$

where φ_a and φ_b are the phase changes of the grating interferometer in the X and Y directions. Δa and Δb are the displacements generated by the 2D grating in the X and Y directions, respectively. Δf_a and Δf_b are the frequency differences of the ± 1 st-order diffracted light generated symmetrically in the X and Y directions, respectively. ρ_x and ρ_y are the grating groove density in the X and Y directions, respectively, with units of grooves/mm (gr/mm) representing the number of grating lines per millimeter, and the grating groove density is the reciprocal of the grating pitch d .

As shown in Fig. 2 (color online), when the 2D grating undergoes a displacement within the plane, because the grating interference signal is generated when the laser cuts the grating lines vertically, the X and Y measurement axes (green) of the grating interferometer are oriented perpendicular to the Y-direction and X-direction grating lines (blue) of the grating, respectively. Under the influence of the orthogonality error of grating grooves α and the grat-

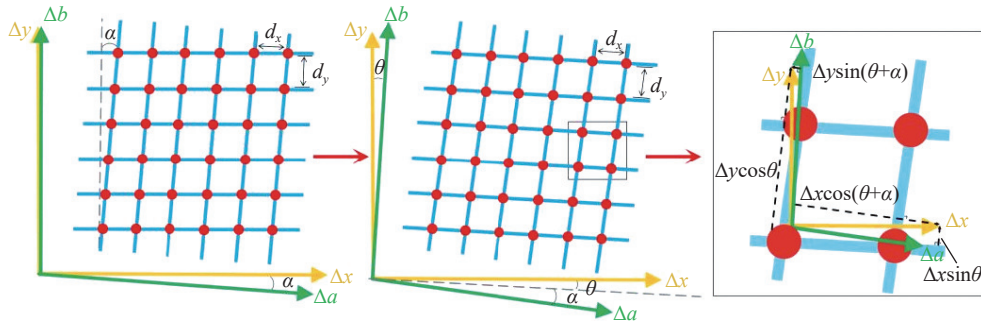


Fig. 2 The influence of orthogonality error of grating grooves error and grating installation error on displacement measurement

The interference phase corresponding to the diffracted light can be expressed as:

$$\begin{bmatrix} \varphi_a \\ \varphi_b \end{bmatrix} = 4\pi \begin{bmatrix} \rho_x \cos(\theta + \alpha) & -\rho_x \sin(\theta + \alpha) \\ \rho_y \sin \theta & \rho_y \cos \theta \end{bmatrix} \begin{bmatrix} \Delta x \\ \Delta y \end{bmatrix}. \quad (8)$$

Analysis of the equation above indicates that the unknowns are the grating installation error θ , the orthogonality error of grating grooves α , and the groove densities ρ_x and ρ_y in the X and Y directions, respectively. Because the number of unknowns is greater than the number of equations, it is not possible to obtain a direct solution. Therefore, at least one more displacement must be introduced to solve for these four parameters, and we have the following:

$$\begin{cases} \varphi_a = 4\pi\rho_x [\Delta x \cos(\theta + \alpha) - \Delta y \sin(\theta + \alpha)] \\ \varphi_b = 4\pi\rho_y (\Delta x \sin \theta + \Delta y \cos \theta) \\ \varphi'_a = 4\pi\rho_x [\Delta x' \cos(\theta + \alpha) - \Delta y' \sin(\theta + \alpha)] \\ \varphi'_b = 4\pi\rho_y (\Delta x' \sin \theta + \Delta y' \cos \theta) \end{cases}. \quad (9)$$

By solving the system of equations above in combination with equations (2) and (3), the grating

installation error θ , an angular deviation occurs between the measurement axes of the grating interferometer and the corresponding measurement axes (yellow) of the laser interferometer. The relationship between the displacement measured by the grating interferometer and the displacement measured by the laser interferometer is given by:

$$\begin{bmatrix} \Delta a \\ \Delta b \end{bmatrix} = \begin{bmatrix} \cos(\theta + \alpha) & -\sin(\theta + \alpha) \\ \sin \theta & \cos \theta \end{bmatrix} \begin{bmatrix} \Delta x \\ \Delta y \end{bmatrix}. \quad (7)$$

installation error θ , the orthogonality error of grating grooves α , and the groove densities ρ_x and ρ_y can be expressed successively as follows:

$$\theta = \arctan \left(\frac{\varphi'_y \varphi_b - \varphi_y \varphi'_b}{\varphi_x \varphi'_b - \varphi'_x \varphi_b} \right), \quad (10)$$

$$\alpha = \arctan \left(\frac{\varphi_x \varphi'_a - \varphi'_x \varphi_a}{\varphi_y \varphi'_a - \varphi'_y \varphi_a} \right) - \theta, \quad (11)$$

$$\rho_x = \frac{n_{\text{air}} \varphi_a}{\lambda [\varphi_x \cos(\theta + \alpha) - \varphi_y \sin(\theta + \alpha)]}, \quad (12)$$

$$\rho_y = \frac{n_{\text{air}} \varphi_b}{\lambda (\varphi_x \sin \theta + \varphi_y \cos \theta)}. \quad (13)$$

3 Experiment and results

The experimental setup is illustrated in Fig. 3 (color online). Both the grating interferometer and the laser interferometer use the same dual-frequency laser (5517D, Keysight) with an operating wavelength of 632.8 nm and a frequency difference of 2.4 MHz as their light source. A self-de-

veloped 2D grating with a grating groove density of 1200 gr/mm, as shown in Fig. 3(c), was measured. This grating was fabricated using holographic exposure technology, with a diffraction efficiency of more than 15%, a surface roughness of better than

$0.2\lambda@632.8\text{ nm}$, and dimensions of $80\text{ mm}\times 80\text{ mm}\times 10\text{ mm}$. A high-precision planar displacement stage (L-731, PI) carries the grating and the measurement mirror to enable movement.

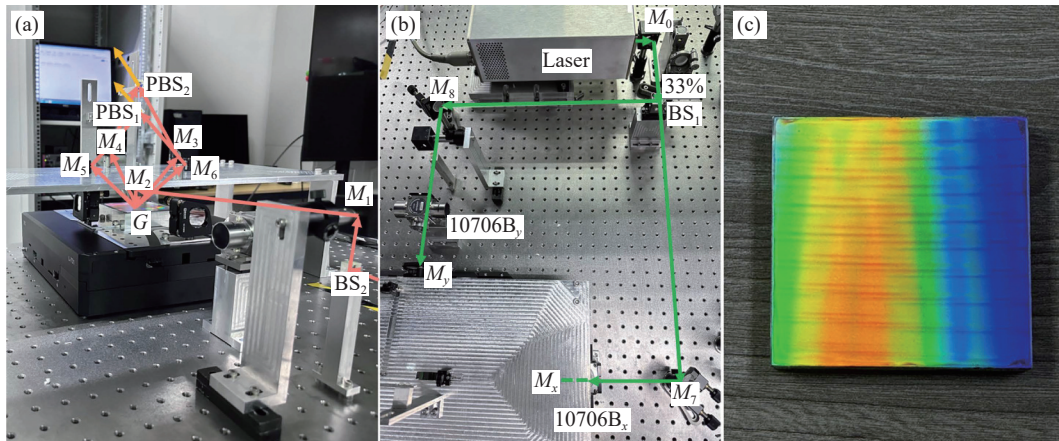


Fig. 3 Experimental device photographs. (a) Layout of the 2D grating interferometer; (b) layout of the laser interferometer; (c) 2D grating

To ensure that the measurement axes of the laser interferometer are coplanar with the surface of the grating to be measured as far as possible and thus reduce the Abbe error, metal bases of the same height were designed and processed to fix the X and Y-axis laser interferometer components. Because the single board can only detect three signals, including the laser reference signal, two data processing boards (N1230A and N1231B, Keysight) are used to cooperate with PD (10780F, Keysight) to achieve synchronous triggering, and four measurement signals are obtained at the same time, which ensures the real-time synchronization of the measurement. During the experiments, the entire measurement device was placed on an air-floating optical platform to reduce the effects of environmental vibrations on the final measurement accuracy.

3.1 Steadiness test

First, the stability of the system was evaluated. During the experiment, the displacement stage remained stationary. The grating interferometer and the laser interferometer collected interference signals continuously at a sampling rate of 500 Hz for 60 s and transmitted these signals to the board for

the displacement calculations. Two environmental monitoring devices were deployed for comprehensive parameter logging: a Fluke Networks L586A sensor for temperature tracking and a Vaisala PTU300 tri-parameter probe simultaneously recording barometric pressure, relative humidity. The recorded values were then substituted into the modified Edlen^[37] empirical formula to correct the air refractive index. Within 60 s in the measurement environment, the Peak to valley(PV) value of the temperature change was measured to be $\pm 0.1\text{ }^{\circ}\text{C}$, the PV value of the pressure was $\pm 50\text{ Pa}$, and the PV value of the humidity change was $\pm 1\%$.

According to the deviation results from the four-channel interferometers shown in Fig. 4 (color online), the displacement deviations of the four-channel interference signals caused by the unstable measurement environment were 11.2 nm, 9.2 nm, 7.5 nm, and 7.7 nm. In the measurement range of 5 mm, this is equivalent to grating groove density errors of $4.48\times 10^{-6}\text{ gr/mm}$ in the X-direction and $4.06\times 10^{-6}\text{ gr/mm}$ in the Y-direction. The corresponding orthogonality error of grating grooves error was approximately 0.6". Because the magnitude

of these three numbers is very small, their influence

on the final measurement results can be ignored.

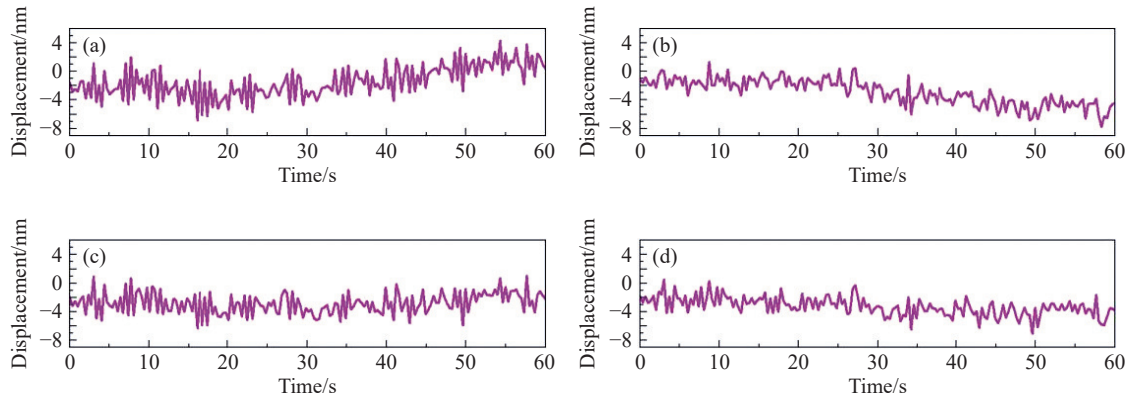


Fig. 4 Stability test result. Values measured by (a) the X-direction laser interferometer and (b) the Y-direction laser interferometer. Measured values from (c) the X-direction grating interferometer and (d) the Y-direction grating interferometer

3.2 Orthogonality measurement of dual-axis laser interferometer

In this experiment, a biaxial laser interferometer was used to provide the true displacement values in the X and Y directions for the 2D displacement stage. When the two measurement axes are not orthogonal, the displacement in the X-axis direction will introduce an additional displacement component into the Y-axis measurement optical path, and vice versa. This seriously affects the measurement accuracy for the grating groove density and orthogonality error of grating grooves. To ensure the measurement accuracy, a high-precision planar displacement stage was used to calibrate the orthogonality of the biaxial laser interferometer. The displacement in the Y-direction when the planar

displacement stage moves along the X-axis and the displacement in the X-direction when the stage moves along the Y-axis were measured. Then, based on the trigonometric function relationship, the orthogonal angle of the biaxial interferometer was corrected.

During the experiments, the displacement stage was made to move by 5 mm along the X and Y directions at a speed of 1 mm/s. The interference signals from the biaxial laser interferometer were recorded continuously and transmitted to the data acquisition module to allow the phase change to be converted into displacement values. Figure 5 (color online) shows the measurement results acquired after averaging the experimental data from five experimental runs.

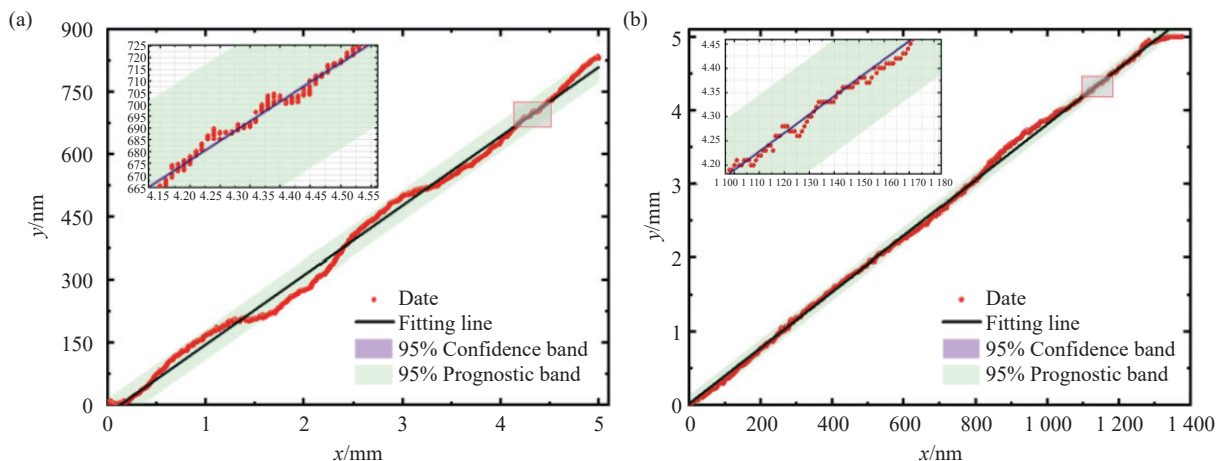


Fig. 5 Linear fitting results for plane displacement platform movement along (a) the X-axis and (b) the Y-axis

The least-squares method was used to process the measurement data from the two axes for linear fitting. The angles between the two fitted lines and the coordinate axes were obtained based on the slopes, and the angular deviations in the X and Y directions were determined to be $34.2616''$ and $54.3372''$, respectively.

3.3 Measuring the impact of regional differentiation

It can be seen from Formula (9) that in the calibration system, the grating must be displaced at least twice in order to simultaneously determine the grating groove density, orthogonality error of grating grooves and grating installation error. When the 2D grating moves within the grating plane, the reading change in the grating scale is only related to the number of grating lines that the grating has moved across, and it is independent of the movement path. Therefore, during the experiment, the grating is moved first in the X-direction and then in the Y-direction. The data acquired from these two movements are then used as a calculation data set.

To verify the effects of the different measurement regions of the grating used in these experiments on the grating groove density measurement results, the displacement stage is driven to move five times at a speed of 0.1 mm/s in both the X and Y directions, starting at the origin and stepping over areas of 1 mm^2 each time. For each step, the data are collected six times. The six data sets are then substituted into equation (9) to perform the calculations, and the differences among the calibration results for the grating groove density at the different positions are compared. The data comparison is shown in Fig. 6 (color online). The center line of the box-plot represents the average of the six measured values from the grating groove density measurements in the two main periodic directions. The length of the box-plot represents the standard error for the confidence level of the average of the measured values. The whisker lines shown above and below the boxes

represent the standard deviation ranges of the measured values.

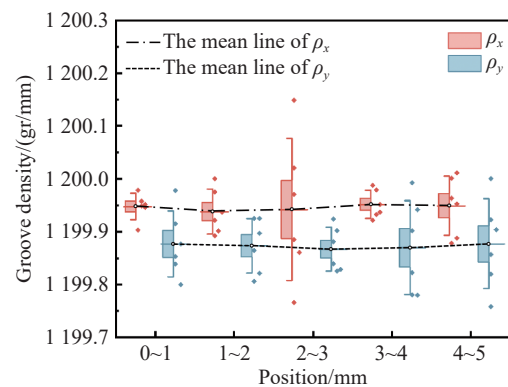


Fig. 6 Grating groove density measurement results

These results show that within the measurement range from 0–5 mm, the standard deviation of the grating groove density in the X-direction is $5.55 \times 10^{-3} \text{ gr/mm}$, and the corresponding value in the Y-direction is $4.43 \times 10^{-3} \text{ gr/mm}$. This is equivalent to introduction of an angular deviation of approximately $1.7''$ into the measurements of the installation error and the orthogonality error of grating grooves. The overall impact on the measurement results is negligible, however.

3.4 Detection of grating groove density and the orthogonality error of grating grooves

To allow the grating groove density and the orthogonality error of grating grooves error of the 2D grating to be measured, the displacement stage moves within the 0–5 mm range during the experiments at a speed of 0.1 mm/s . Similar to the previous measurements, the grating is moved first in the X-direction and then in the Y-direction. The data from these two movements are then used as a calculation data set, denoted by (x_n, y_n) .

An overall full-format evaluation is conducted in the form of the grid shown in Fig. 7 (color online), which is more in line with an actual application scenario for the metrological 2D grating. Data collection is performed according to the displacements for the nine different distances listed in Table 1, and the data for each displacement are collected six times.

The six data collected in the X-direction and

the six data collected in the Y-direction for each displacement are grouped in pairs. Through permutation and combination processes, 36 calculation data sets are obtained. These data are then substituted into equation (9) to perform the required calculations to average out the influence of the errors and improve the accuracy of the final calculation results. Figure 8 (color online) shows the 36 sets of calculation results that were obtained from each displacement measurement, along with their average values.

The results obtained from the nine different displacements were averaged again, and the final measurement results are listed in Table 1.

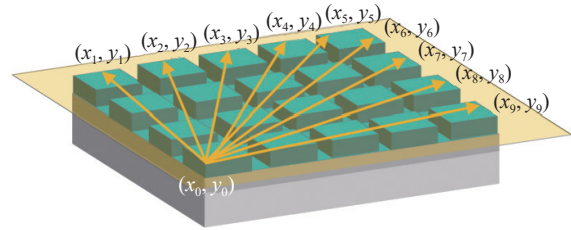


Fig. 7 Schematic diagram of the measurement path

Tab. 1 The solution results of the parameters to be measured

(x_n, y_n)	$\theta(^{\circ})$	$\alpha(^{\circ})$	$\rho_x(\text{gr/mm})$	$\rho_y(\text{gr/mm})$
(1,5)	0.48016	-1.07329	1199.99228	1199.90331
(2,5)	0.48820	-1.08118	1199.99563	1199.90466
(3,5)	0.48496	-1.07812	1200.02361	1199.90413
(4,5)	0.48669	-1.07981	1200.02964	1199.90443
(5,5)	0.48652	-1.07963	1200.01899	1199.90439
(5,4)	0.48654	-1.07839	1200.01872	1199.87662
(5,3)	0.48653	-1.07917	1200.01889	1199.88735
(5,2)	0.48668	-1.06947	1200.01681	1199.88468
(5,1)	0.48653	-1.07342	1200.01767	1199.87282
Average value	0.48587	-1.07694	1200.01469	1199.89360
Standard deviation	0.002158	0.003702	0.01171085	0.01322980

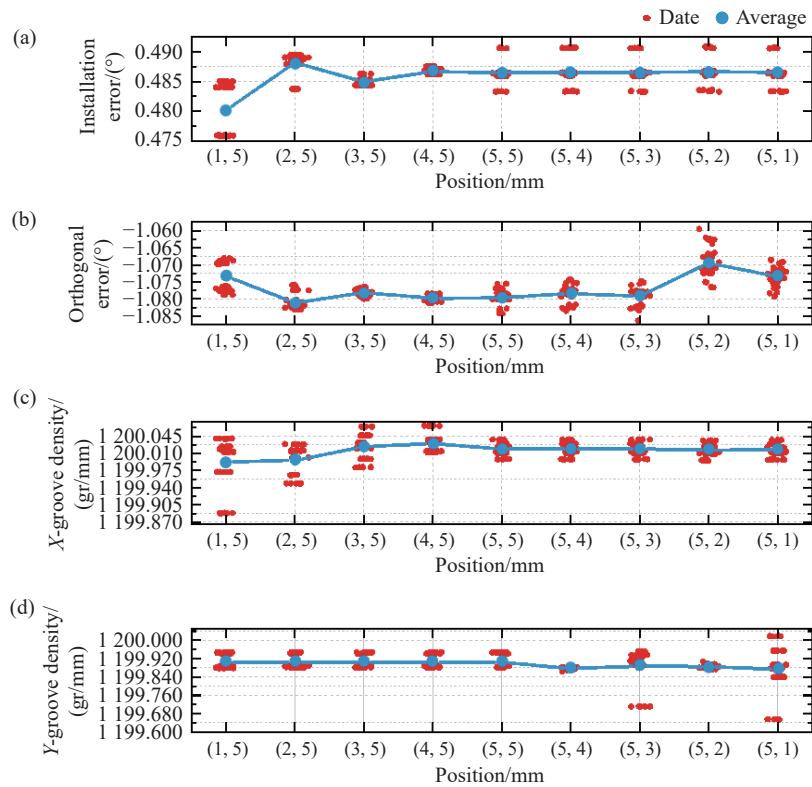


Fig. 8 Data solution results. (a) Grating installation error; (b) orthogonality error for the grating lines; (c) X-direction grating groove density; (d) Y-direction grating groove density

The experimental results show that the installation error measured via this method is 0.48587° , with a standard deviation of better than 0.003° . The orthogonality error of grating grooves is -1.07694° , with a standard deviation of better than 0.004° . The X-and Y-direction groove densities are 1200.01469 gr/mm and 1199.8936 gr/mm , and their standard deviations are better than 0.012 gr/mm and 0.014 gr/mm , respectively.

3.5 Contrast experiment

To verify the accuracy of the measurement results, the calibration results for the grating groove

density and the orthogonality error of grating grooves were compared with those obtained by the AFM method for the same grating. The measurement principle used is to filter the raster data obtained by scanning and then determine the grating pitch by calculating its spatial frequency within the frequency domain^[25]. Figure 9(a) (color online) shows a $512 \text{ pixel} \times 512 \text{ pixel}$ 2D grating raster image obtained using an atomic force microscope within a $50 \mu\text{m} \times 50 \mu\text{m}$ range at a sampling frequency of 0.3 Hz .

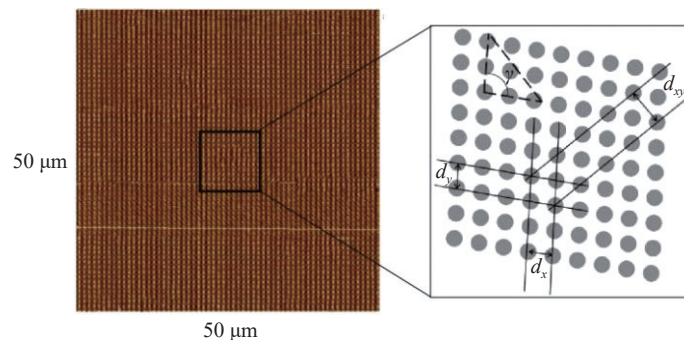


Fig. 9 The AFM image and data acquisition schematic diagram of 2D grating. (a) Measured images of AFM; (b) data acquisition

At the same time, to determine the orthogonality error of grating grooves of the 2D grating, data collection must be performed in the manner shown in Fig. 9(b) (color online). Then, by substituting the average grating pitches in each direction obtained after Fourier transformation, which are denoted by d_x , d_y , and d_{xy} , into the cosine theorem, the orthogonality characteristics of the 2D grating can be calculated.

During the verification process using the AFM method, the orthogonality error of grating grooves and the grating groove density were measured by intercepting and measuring the data within five different rectangular regions with dimensions of $10 \mu\text{m} \times 10 \mu\text{m}$, and the results are shown in Table 2. The experimental results prove that the orthogonality error of grating grooves measured via the AFM method is -1.0735° , with a standard deviation of better than 0.003° . The groove densities in the X and Y direc-

tions are 1200.0189 gr/mm and 1199.9277 gr/mm , and the corresponding standard deviations are better than 0.017 gr/mm and 0.018 gr/mm , respectively.

Tab. 2 The results of the measurement of the 2D grating calibration area

Measuring field	$\alpha(^{\circ})$	$\rho_x(\text{gr/mm})$	$\rho_y(\text{gr/mm})$
1	-1.07126	1200.03871	1199.94367
2	-1.07313	1199.99825	1199.92325
3	-1.07493	1200.01830	1199.92155
4	-1.07138	1200.00781	1199.94672
5	-1.07653	1200.03141	1199.90339
Average value	-1.07345	1200.01890	1199.92771
Standard deviation	0.002284	0.016573373	0.017786239

When the results obtained by the AFM method are compared with those measured by the method proposed in this paper, as the results shown in

Fig. 10 (color online), the differences in the grating groove density are 0.0042 gr/mm and 0.034 gr/mm in the X and Y directions, respectively, and the difference in the orthogonality error of grating grooves is 0.00349°. In addition, the consistencies of the

groove densities in the X and Y directions are better than 0.03 gr/mm and 0.06 gr/mm, respectively, and the consistency of the orthogonality error of grating grooves is better than 0.008°.

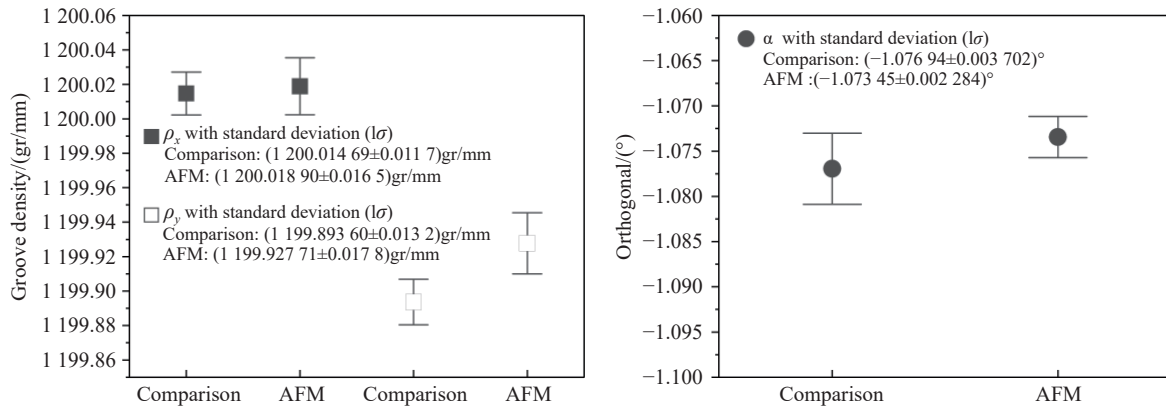


Fig. 10 Comparison of results for the two measurement methods. (a) Comparison of grating groove density measurement results; (b) comparison of orthogonality error of grating grooves error results

The possible reasons for the differences between the measurement results obtained by the two methods are discussed as follows. First, the measurement range of the laser interferometer is much greater than that of the atomic force microscope. As a result, the average effects represented by the measurement results from the two methods are different. Second, there may be minor undulations and/or contaminants on the sample surface. These factors can affect the shapes of the interference fringes or the contact and the interaction force between the AFM probe and the sample surface, thus causing slight deviations in the measurement results.

4 Conclusion

This paper presents a method to perform simultaneous calibration of the grating groove density and the orthogonality error of grating grooves of a 2D grating using a heterodyne orthogonal laser interferometer. Calibration experiments were conducted on a self-made 1200 gr/mm 2D grating in the laboratory. The standard deviations for the grating groove density in the X and Y directions were better than

0.012 gr/mm and 0.014 gr/mm, respectively, and the standard deviation for the orthogonality error of grating grooves was -1.07694° with a standard deviation of less than 0.004° . The AFM method was combined with the Fourier analysis method to verify the accuracy of the proposed method. The consistencies of the grating groove density in the X direction and Y direction were better than 0.03 gr/mm and 0.06 gr/mm, respectively, and the consistency of the orthogonality error of grating grooves was better than 0.008° . At present, the technique proposed in this paper only calibrates gratings with a grating groove density of 1200 gr/mm. In future work, the optical path structure will be improved by increasing the adjustment freedom of the turning mirror to meet the calibration requirements of gratings with different groove densities. In addition, this paper only uses a method based on well-posed equations to solve for multiple parameters. Subsequently, an over-determined equation system will be constructed in future work based on multiple displacement measurement data to reduce the impact of the grating pitch uniformity error on the calibration accuracy.

References:

- [1] GAO W, KIM S W, BOSSE H, *et al.*. Measurement technologies for precision positioning[J]. *CIRP Annals*, 2015, 64(2): 773-796.
- [2] 谭久彬. 超精密测量与高端装备制造质量[J]. 中国工业和信息化, 2020(6): 18-23.
TAN J B. Ultra-precision measurement and high-end equipment manufacturing quality[J]. *China Industry & Information Technology*, 2020(6): 18-23. (in Chinese).
- [3] BUTLER H. Position control in lithographic equipment: an enabler for current-day chip manufacturing[J]. *IEEE Control Systems Magazine*, 2011, 31(5): 28-47.
- [4] 王磊杰, 张鸣, 朱煜. 单体大尺寸高精度全息光栅制造技术综述[J]. *光学精密工程*, 2021, 29(8): 1759-1768.
WANG L J, ZHANG M, ZHU Y. Review of monomeric large-size and high precision holographic planar grating manufacturing technology[J]. *Optics and Precision Engineering*, 2021, 29(8): 1759-1768. (in Chinese).
- [5] 王磊杰, 张鸣, 朱煜, 等. 面向浸没式光刻机的超精密光学干涉式光栅编码器位移测量技术综述[J]. *光学精密工程*, 2019, 27(9): 1909-1918.
WANG L J, ZHANG M, ZHU Y, *et al.*. Review of ultra-precision optical interferential grating encoder displacement measurement technology for immersion lithography scanner[J]. *Optics and Precision Engineering*, 2019, 27(9): 1909-1918. (in Chinese).
- [6] AL-RAWASHDEH Y M, AL JANAIDEH M, HEERTJES M F. Kinodynamic generation of wafer scanners trajectories used in semiconductor manufacturing[J]. *IEEE Transactions on Automation Science and Engineering*, 2023, 20(1): 718-732.
- [7] 李星辉, 崔璨. 光栅干涉精密纳米测量技术[J]. *光学精密工程*, 2024, 32(17): 2591-2611.
LI X H, CUI C. Grating interferometric precision nanometric measurement technology[J]. *Optics and Precision Engineering*, 2024, 32(17): 2591-2611. (in Chinese).
- [8] ZHOU W Y, SUN Y J, LIU ZH W, *et al.*. A random angle error interference eliminating method for grating interferometry measurement based on symmetry Littrow structure[J]. *Laser & Photonics Reviews*, 2025, 19(11): 2401659.
- [9] 冯灿. 平面位移测量用二维衍射光栅的标定方法[D]. 北京: 清华大学, 2012.
FENG C. *Calibration method of two-dimensional diffraction gratings used for planar displacement measurement*[D]. Beijing: Tsinghua University, 2012. (in Chinese).
- [10] YACOOT A, KOENDERS L. Recent developments in dimensional nanometrology using AFMs[J]. *Measurement Science and Technology*, 2011, 22(12): 122001.
- [11] SHENG B, CHEN G H, HUANG Y SH, *et al.*. Measurement of grating groove density using multiple diffraction orders and one standard wavelength[J]. *Applied Optics*, 2018, 57(10): 2514-2518.
- [12] LEI L H, LIU Y, CHEN X, *et al.*. Fast and accurate calibration of 1D and 2D gratings[J]. *Advanced Materials Research*, 2011, 317-319: 2196-2203.
- [13] KOROTKOV V I, PULKIN S A, VITUSHKIN A L, *et al.*. Laser interferometric diffractometry for measurements of diffraction grating spacing[J]. *Applied Optics*, 1996, 35(24): 4782-4786.
- [14] VITUSHKIN L F, ZEILIKOVICH I S, KOROTKOV V I, *et al.*. High-precision measurements of the groove spacing of diffraction gratings using the interference diffractometer and study of the quality of diffraction gratings[J]. *Optics and Spectroscopy*, 1994, 77(1): 129-135.
- [15] ISRAEL W, TIEMANN I, METZ G, *et al.*. An international length comparison at an industrial level using a photoelectric incremental encoder as transfer standard[J]. *Precision Engineering*, 2003, 27(2): 151-156.
- [16] SAWABE M, MAEDA F, YAMARYO Y, *et al.*. A new vacuum interferometric comparator for calibrating the fine linear encoders and scales[J]. *Precision Engineering*, 2004, 28(3): 320-328.
- [17] TIEMANN I, SPAETH C, WALLNER G, *et al.*. An international length comparison using vacuum comparators and a photoelectric incremental encoder as transfer standard[J]. *Precision Engineering*, 2008, 32(1): 1-6.
- [18] KIM J A, KIM J W, PARK B C, *et al.*. Measurement of microscope calibration standards in nanometrology using a metrological atomic force microscope[J]. *Measurement Science and Technology*, 2006, 17(7): 1792-1800.
- [19] KIM J A, KIM J W, PARK B C, *et al.*. Calibration of two-dimensional nanometer gratings using optical diffractometer and metrological atomic force microscope[J]. *Proceedings of SPIE*, 2005, 5879: 58790Z.
- [20] KIM J A, KIM J W, KANG C S, *et al.*. Measurements of two-dimensional gratings using a metrological atomic force

- microscope with uncertainty evaluation[J]. *International Journal of Precision Engineering and Manufacturing*, 2008, 9(2): 18-22.
- [21] DIXSON R, ORJI N G, FU J, *et al.*. Traceable atomic force microscope dimensional metrology at NIST[J]. *Proceedings of SPIE*, 2006, 6152: 61520P.
- [22] MISUMI I, GONDA S, KUROSAWA T, *et al.*. Uncertainty in pitch measurements of one-dimensional grating standards using a nanometrological atomic force microscope[J]. *Measurement Science and Technology*, 2003, 14(4): 463-471.
- [23] MELI F, THALMANN R. Long-range AFM profiler used for accurate pitch measurements[J]. *Measurement Science and Technology*, 1998, 9(7): 1087-1092.
- [24] JORGENSEN J F, JENSEN C P, GARNAES J. Lateral metrology using scanning probe microscopes, 2D pitch standards and image processing[J]. *Applied Physics A*, 1998, 66(S1): S847-S852.
- [25] DAI G L, KOENDERS L, POHLENZ F, *et al.*. Accurate and traceable calibration of one-dimensional gratings[J]. *Measurement Science and Technology*, 2005, 16(6): 1241-1249.
- [26] MISUMI I, GONDA S, KUROSAWA T, *et al.*. Submicrometre-pitch intercomparison between optical diffraction, scanning electron microscope and atomic force microscope[J]. *Measurement Science and Technology*, 2003, 14(12): 2065-2074.
- [27] EVES B J, PEKELSKY J R, DECKER J E. Uncertainty evaluation of the NRC imaging diffractometer[J]. *Measurement Science and Technology*, 2008, 19(7): 075103.
- [28] MELI F, THALMANN R, BLATTNER P. High precision pitch calibration of gratings using laser diffractometry[C]. *Bremen, Germany: Shaker Verlag*, 1999: 252-255.
- [29] DAI G L, POHLENZ F, DZIOMBA T, *et al.*. Accurate and traceable calibration of two-dimensional gratings[J]. *Measurement Science and Technology*, 2007, 18(2): 415-421.
- [30] NOBACH H, DAMASCHKE N, TROPEA C. High-precision sub-pixel interpolation in particle image velocimetry image processing[J]. *Experiments in Fluids*, 2005, 39(2): 299-304.
- [31] WOO W H, YEN K S. Moiré fringe center determination using artificial neural network[J]. *Proceedings of SPIE*, 2015, 9631: 96312B.
- [32] GARNAES J, DIRSCHERL K. NANO5—2D grating—final report[J]. *Metrologia*, 2008, 45(1A): 04003.
- [33] FENG C, KAJIMA M, GONDA S, *et al.*. Accurate measurement of orthogonality of equal-period, two-dimensional gratings by an interferometric method[J]. *Metrologia*, 2012, 49(3): 236-244.
- [34] XIE Y F, JIA W, ZHAO D, *et al.*. Traceable and long-range grating pitch measurement with picometer resolution[J]. *Optics Communications*, 2020, 476: 126316.
- [35] HSU C C, TSAI C M, YE CH Y, *et al.*. Period measurement of a periodic structure by using a heterodyne grating interferometer[J]. *Applied Optics*, 2024, 63(15): 4211-4218.
- [36] 董欣媛, 孙双花, 崔京远, 等. 基于正交双轴激光干涉仪的二维光栅校准系统误差分析[J]. *计量学报*, 2019, 40(6A): 36-41.
- DONG X Y, SUN SH H, CUI J Y, *et al.*. Error analysis of two-dimensional grating calibration system based on orthogonal dual-axis laser interferometer[J]. *Acta Metrologica Sinica*, 2019, 40(6A): 36-41. (in Chinese).
- [37] BIRCH K P, DOWNS M J. An updated Edlén equation for the refractive index of air[J]. *Metrologia*, 1993, 30(3): 155-162.

Author Biographies:



TENG Hai-rui (2000—), master graduate student, received a bachelor degree from Ludong University in 2018. He is currently studying for a master degree in Changchun Institute of Optics and Mechanics, Chinese Academy of Sciences. He is mainly engaged in grating displacement measurement and 2D grating calibration. E-mail: tenghairui22@mails.ucas.ac.cn



LIU Zhao-wu (1979—), Ph.D., received his doctor degree from Changchun Institute of Optics and Machines, Chinese Academy of Sciences in 2017. He is currently an associate researcher at Changchun Institute of Optics and Machines, Chinese Academy of Sciences, mainly engaged in grating displacement measurement technology research. E-mail: zhaowuliu@ciomp.ac.cn